# Soliton Interactions of the Kadomtsev–Petviashvili Equation and Generation of Large-Amplitude Water Waves

*By G. Biondini, K.-I. Maruno, M. Oikawa, and H. Tsuji*

We study the maximum wave amplitude produced by line-soliton interactions of the Kadomtsev–Petviashvili II (KPII) equation, and we discuss a mechanism of generation of large amplitude shallow water waves by multi-soliton interactions of KPII. We also describe a method to predict the possible maximum wave amplitude from asymptotic data. Finally, we report on numerical simulations of multi-soliton complexes of the KPII equation which verify the robustness of all types of soliton interactions and web-like structure.

## 1. Introduction

The existence of waves of large height on the sea surface is a dangerous phenomenon [1–6]. Extreme waves occur much more frequently than it might be expected from surface wave statistics [2]. These extreme waves, which are particularly steep and may arise both in deep water and in shallow water, have a significant impact on the safety of people and infrastructure, and are responsible for the erosion of coastlines and sea bottoms and changes to the biological environment. Thus, understanding the physics of these extreme waves is an important task which may even contribute to save lives. Although

Address for correspondence: G. Biondini, State University of New York, Buffalo, NY 14260-4500, USA; e-mail: biondini@buffalo.edu

*STUDIES IN APPLIED MATHEMATICS* 122:377–394

several physical mechanisms of generation of extreme waves in deep water have been studied, less is known for the situation of shallow water [4].

Waves in shallow water have been studied since the nineteenth century, of course. It is well-known that, in the case of weak nonlinearity, for weakly two-dimensional cases (that is, for the cases that the scale of variation in the direction normal to the propagation direction is much longer than that in the propagation direction) the fundamental equations for the dynamics in shallow water may be reduced to the Kadomtsev–Petviashvili II (KPII) equation [7–9]. Because the KP equation is integrable, the theory of integrable system can be used to analyze wave dynamics in detail. In particular, Soomere et al. recently studied the amplitude of ordinary 2-soliton solutions of the KPII equation [10–12]. They pointed out that the interaction of two solitary waves may be one mechanism of generation of extreme waves. In the case of ordinary 2-soliton solutions, the maximum interaction height can be four times that of the incoming solitary waves, as in the case of the resonant Y-shaped solution originally found by Miles [13–15]. The interaction pattern of the Miles solution and ordinary 2-soliton solutions, however, is stationary. Therefore, it cannot describe how a large amplitude wave can be generated. Recently, we studied a class of exact line soliton solutions of the KPII equation and found nonstationary interaction patterns and web-like structures [16]. Such solutions describe resonant line-soliton interactions, which are generalization of the Y-shaped resonant soliton solution. More general solutions were later characterized in [17–21].

Our motivation in this paper is severalfold: (i) we determine the maximum amplitude in interactions of line solitons of the KPII equation, (ii) we propose a mechanism to explain the generation of waves of large height, (iii) we describe an algorithm to determine the maximum amplitude from experimental data, (iv) we perform numerical simulations of multi-soliton interactions of the KPII equation, whose results confirm the robustness and stability of soliton interactions and web-like structure.

## 2. The KPII equation and its soliton solutions

Here we briefly review some essential results the KPII equation

$$(-4u_t + 6uu_x + u_{xxx})_x + 3u_{yy} = 0 \tag{1}$$

that will be referred to through the remaining of this work. Hereafter, $u(x, y, t)$ represents the dimensionless wave height to leading order, and subscripts $x$, $y$, $t$ denote partial differentiation. It is well known that solutions of (1) can be expressed via a tau function $\tau(x, y, t)$ as

$$u(x, y, t) = 2\frac{\partial^2}{\partial x^2} \log \tau(x, y, t), \tag{2}$$

where $\tau(x, y, t)$ satisfies Hirota's bilinear equation [22, 23]. Solutions of Hirota's equation can be written in terms of the Wronskian determinant [24, 25]

$$\tau(x, y, t) = \mathrm{Wr}(f_1, \ldots, f_N) = \det\left(f_n^{(n'-1)}\right)_{1\le n,n'\le N}, \tag{3}$$

with $f_n^{(j)} = \partial^j f_n/\partial x^j$, and where $f_1, \ldots, f_N$ are a set of linearly independent solutions of the linear system

$$\frac{\partial f}{\partial y} = \frac{\partial^2 f}{\partial x^2}, \quad \frac{\partial f}{\partial t} = \frac{\partial^3 f}{\partial x^3}. \tag{4}$$

For example, ordinary $N$-soliton solutions are obtained by taking $f_n = e^{\theta_{2n-1}} + e^{\theta_{2n}}$ for $n = 1, \ldots, N$, where

$$\theta_m(x, y, t) = -k_m x + k_m^2 y - k_m^3 t + \theta_{m;0} \tag{5}$$

for $m = 1, \ldots, 2N$, where the $4N$ parameters $k_1 < \cdots < k_{2N}$ and $\theta_{1;0}, \ldots, \theta_{2N;0}$ are real constants. For $N = 1$, one obtains the single-soliton solution of KPII:

$$u_{i,j}(x, y, t) = \tfrac{1}{2}a_{i,j}^2 \operatorname{sech}^2\left[\tfrac{1}{2}(\theta_i - \theta_j)\right] \tag{6}$$

where $i = 1$ and $j = 2$. Equation (6) is a traveling-wave solution [with wavenumber $\mathbf{k} = (k_j - k_j, k_i^2 - k_j^2)$ and frequency $\omega = k_i^3 - k_j^3$], exponentially localized along the line $\theta_i = \theta_j$ of the $xy$-plane, and is therefore referred to as a *line soliton*. We refer to

$$a_{i,j} = k_j - k_i\,, \qquad d_{i,j} = k_i + k_j \tag{7}$$

respectively, as the soliton *amplitude* and *direction*. Note that $d_{i,j} = \tan\alpha_{i,j}$, where $\alpha_{i,j}$ is the angle made by the soliton with the positive $y$-axis (counted clockwise), because $\theta_i - \theta_j = (k_i - k_j)[-x + d_{i,j}\, y - (k_i^2 + k_i k_j + k_j^2)t] + \theta_{i;0} - \theta_{j;0}$. The actual maximum of the solution, or wave height, is given by $U_{i,j} = \frac{1}{2}a_{i,j}^2$.

The case with $N = 1$ and $f = e^{\theta_1} + \cdots + e^{\theta_M}$, with $\theta_1, \ldots, \theta_M$ still given by (5), was studied in [26]. In particular $M = 3$ yields the Y-shaped solution often called *Miles resonance*, in which three line solitons interact at a vertex, as shown in Figure 1, and whose wavenumbers and phase parameters satisfy the resonance conditions $\mathbf{k}_1 + \mathbf{k}_2 = \mathbf{k}_3$ and $\omega_1 + \omega_2 = \omega_3$. (Note that, while the Miles resonance is also a traveling-wave solutions, solutions with $M \ge 4$ are not [26].) More in general, choosing $f_n = f^{(n-1)}$ for $n = 1, \ldots, N$ yields $\tau(x, y, t)$ in the form of a Hankel determinant. In [16] we studied such solutions with $f = e^{\theta_1} + \cdots + e^{\theta_M}$, and we showed that they produce nonstationary and fully resonant $(N_-, N_+)$-soliton solutions of KPII, that is, solutions with $N_- = M - N$ solitons asymptotically as $y \to -\infty$ and $N_+ = N$ solitons asymptotically as $y \to \infty$, and for intermediate values of $y$ these solitons interact resonantly, i.e., via fundamental Miles resonances.

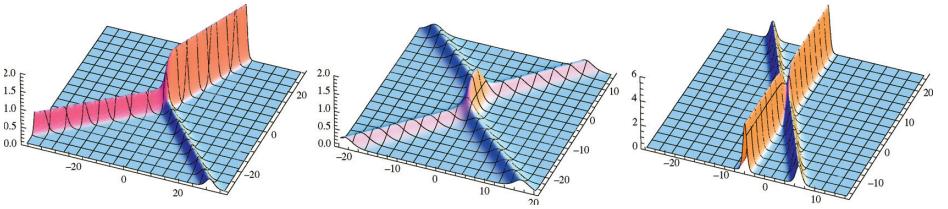

Figure 1. Left: Miles resonance, with $(k_1, k_2, k_3) = (-1.5, 0, 1)$ and $t = 0$. Center: ordinary 2-soliton solution, with $(k_1, \ldots, k_4) = (-1, -0.001, 0, 1)$ and $t = 1$. Right: asymmetric 2-soliton solution, with $(k_1, \ldots, k_4) = (-2, -1.5, 1, 2)$ and $t = 1$. In all cases $\theta_{m;0} = 0$ for $m = 1, \ldots, M$.

More general solutions exist, however. The most general linear combination of exponentials can be written as

$$f_n = \sum_{m=1}^{M} c_{n,m}\, e^{\theta_m} \tag{8}$$

with $\theta_m$ given by (5) as before. Then (3) is expanded as a sum of exponentials:

$$\tau(x, y, t) = \det(C\Theta K) = \sum_{1 \le m_1 < \cdots < m_N \le M} V_{m_1,\ldots,m_N}\, C_{m_1,\ldots,m_N}\, \exp\, \theta_{m_1,\ldots,m_N} \tag{9}$$

where $C = (c_{n,m})$ is the $N \times M$ coefficient matrix, $\Theta = \operatorname{diag}(e^{\theta_1}, \ldots, e^{\theta_M})$, and the $M \times N$ matrix $K$ is given by $K = (k_m^{n-1})$. Hereafter, $\theta_{m_1,\ldots,m_N}$ denotes the phase combination $\theta_{m_1,\ldots,m_N}(x, y, t) = \theta_{m_1} + \cdots + \theta_{m_N}$, while $V_{m_1,\ldots,m_N}$ is the Vandermonde determinant $V_{m_1,\ldots,m_N} = \prod_{1 \le j < j' \le N} (k_{m_{j'}} - k_{m_j})$, and $C_{m_1,\ldots,m_N}$ is the $N \times N$-minor whose $n$th column is, respectively, given by the $m_n$th column of the coefficient matrix for $n = 1, \ldots, N$. The only time dependence in the tau function comes from the exponential phases $\theta_{m_1,\ldots,m_N}$. Also, for all $G \in \mathrm{GL}(N, \mathbb{R})$, the coefficient matrices $C$ and $C' = G\,C$ produce the same solution of KPII. Thus without loss of generality one can consider $C$ to be in row-reduced echelon form (RREF), which we will do throughout this work. One can also multiply each column of $C$ by an arbitrary positive constant which can be absorbed in the definition of $\theta_{1;0}, \ldots, \theta_{M;0}$.

Real nonsingular (positive) solutions of KPII are obtained if $k_1 < \cdots < k_M$ and all minors of $C$ are nonnegative. In [18], we showed that, under these assumptions and some fairly general irreducibility conditions on the coefficient matrix, (9) produces $(N_-, N_+)$-soliton solutions of KPII with $N_- = M - N$ and $N_+ = N$, as in the simpler case of fully resonant solutions. Asymptotic line solitons are given by (6) with the indices $i$ and $j$ labeling the phases $\theta_i$ and $\theta_j$ being swapped in the transition between two dominant phase combinations along the line $\theta_i = \theta_j$. Asymptotic solitons can thus be uniquely characterized by an index pair $[i, j]$ with $1 \le i < j \le M$. We call *outgoing* line solitons

those asymptotic as $y \to \infty$ and *incoming* line solitons those asymptotic as $y \to -\infty$. The index pairs are uniquely identified by appropriate rank conditions on the minors of the coefficient matrix [18]. We also showed in [18] that this decomposition is time-independent, and that the outgoing solitons are identified by pairs $[i_n^+, j_n^+]$, $n = 1, \ldots, N$, where $i_1^+, \ldots, i_N^+$ label the $N$ pivot columns of $C$; similarly, the incoming solitons are identified by pairs $[i_n^-, j_n^-]$, $n = 1, \ldots, M - N$, where $j_1^-, \ldots, j_{M-N}^-$ label the $M - N$ nonpivots columns of $C$.

In general, these solutions exhibit a mixture of resonant and nonresonant interaction patterns. In the special case $M = 2N$, leading to $N_- = N_+ = N$, we call *elastic* $N$-soliton solutions those for which the amplitudes and directions of the incoming solitons coincide with those of the outgoing solitons, while all other $N$-soliton solutions are referred to as *inelastic*. Elastic $N$-soliton solutions were characterized in [17, 21]. The fully resonant line soliton solutions studied in [16] are a special case of the tau function (9) in which all $N \times N$ minors of the coefficient matrix are nonzero.

## 3. Interaction amplitudes of line-soliton solutions

Here we study the amplitude of the interaction arms generated by 2-soliton interactions. These are obtained for $N = 2$ and $M = 4$, yielding the tau function

$$\begin{aligned}\tau(x, y, t) = {} & V_{1,2}C_{1,2}e^{\theta_{1,2}} + V_{1,3}C_{1,3}e^{\theta_{1,3}} + V_{1,4}C_{1,4}e^{\theta_{1,4}} + V_{2,3}C_{1,3}e^{\theta_{2,3}} \\ & + V_{2,4}C_{1,4}e^{\theta_{2,4}} + V_{3,4}C_{3,4}e^{\theta_{3,4}}\,,\end{aligned} \tag{10}$$

where now $V_{i,j} = k_j - k_i$, and with $k_1 < \cdots < k_4$ as before. The 2-soliton solutions of KPII were first classified in [28].

### 3.1. Elastic 2-soliton interactions

It was shown in [21] that elastic 2-soliton solutions divide into three classes, shown in Figures 1 and 2: ordinary (O-type), asymmetric (P-type) and resonant (T-type). The coefficient matrices corresponding to these classes have the following RREFs:

$$C_{\mathrm{O}} = \begin{pmatrix} 1 & 1 & 0 & 0 \\ 0 & 0 & 1 & 1 \end{pmatrix}, \quad C_{\mathrm{P}} = \begin{pmatrix} 1 & 0 & 0 & -1 \\ 0 & 1 & 1 & 0 \end{pmatrix}, \quad C_{\mathrm{T}} = \begin{pmatrix} 1 & 0 & -1 & -1 \\ 0 & 1 & c_{2,3} & c_{2,4} \end{pmatrix}, \tag{11}$$

with $c_{2,3} > c_{2,4} > 0$. These three types of solutions cover disjoint sectors of the 2-soliton parameter space of amplitudes and directions [17]. Moreover, their interaction properties are also different. This difference is obvious in the case of resonant solutions, but also applies to ordinary and asymmetric solutions, because asymmetric solutions only exist for unequal amplitude, and the interaction phase shift has the opposite sign for ordinary and asymmetric

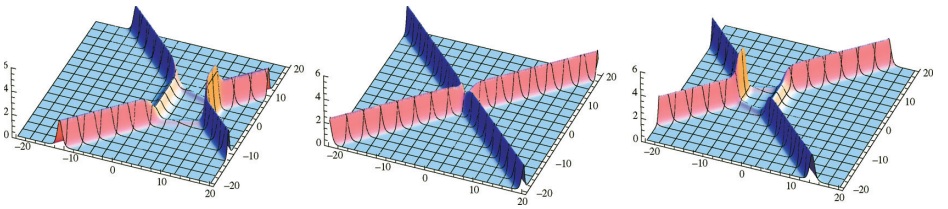

Figure 2. Time evolution of a resonant 2-soliton solution, with $(k_1, \ldots, k_4) = (-2, -1, 1, 2)$ and $\theta_{m;0} = 0$ for $m = 1, \ldots, 4$. Left: $t = -3$; center: $t = 0$; right: $t = 2$.

solutions [17]. We next show that these solutions also differ in terms of the interaction amplitudes.

3.1.1. *Ordinary 2-soliton interactions.* For the coefficient matrix $C_{\mathrm{O}}$ in (11), it is $C_{1,2} = C_{3,4} = 0$, while all other minors are unity. In this case, the dominant phase combination as $x \to -\infty$ is (2, 4) [meaning that $e^{\theta_{2,4}}$ is the dominant exponential in (10)], while that as $x \to \infty$ is (1, 3). The asymptotic solitons are [8, 17] and [18, 19]. The interaction arm corresponds to the double-phase transition (1, 3) $\leftrightarrow$ (2, 4) among the dominant phases in the $xy$-plane, which is located along the line $\theta_{1,3} = \theta_{2,4}$. In a neighborhood of the line corresponding to the double-phase transition $(i_1, i_2) \leftrightarrow (j_1, j_2)$, the tau function and the corresponding solution of KP are approximately, up to exponentially smaller terms,

$$\tau_{i_1 i_2, j_1 j_2}(x, y, t) = V_{i_1, i_2} e^{\theta_{i_1, i_2}} + V_{i_1, j_2} e^{\theta_{j_1, j_2}} \tag{12}$$

and

$$u_{i_1 i_2, j_1 j_2}(x, y, t) = \tfrac{1}{2} a^2_{i_1 i_2, j_1 j_2} \operatorname{sech}^2 \left[ \tfrac{1}{2} (\theta_{j_1, j_2} - \theta_{i_1, i_2} + \Delta_{i_1 i_2, j_1 j_2}) \right] \tag{13}$$

where $\Delta_{i_1 i_2, j_1 j_2} = \log(V_{j_1, j_2} / V_{i_1, i_2})$ and

$$a_{i_1 i_2, j_1 j_2} = k_{j_1} + k_{j_2} - (k_{i_1} + k_{i_2}) = a_{i_1, j_1} + a_{i_2, j_2} \tag{14}$$

and with $a_{i,j}$ given by (7) as before. The interaction arm of ordinary 2-soliton solutions is given by $u(x, y, t) = u_{13,24}(x, y, t)$. Note that $a_{13,24} = a_{1,2} + a_{3,4}$. Thus, the amplitude of the interaction arm is always equal to the sum of the amplitudes of the interacting solitons. Its height is $U_{\max} = \frac{1}{2} a^2_{13,24} > \frac{1}{2}(a^2_{1,2} + a^2_{3,4})$. That is, the height of the interaction arm is always greater than the sum of the heights of the asymptotic solitons. The maximum of this height relative to the height of the individual solitons is obtained in the specal case of equal-amplitude solitons, that is for $a_{1,2} = a_{3,4} =: a$, when $U_{\max} = 2a^2$. Thus the maximum possible amplitude is four times that of the asymptotic solitons. These results are identical to what happens for Y-shape resonant solutions. Note, however, that the double-soliton (13) is *not* by itself an exact solution of the KPII equation (and hence it is not

a true line soliton), because its wavevector and frequency do not satisfy the soliton dispersion relation [27]. This relation is satisfied in the limit $k_3 - k_2 \to 0^+$. In this limit, however, there are only three phases in the tau function, and the solution degenerates to a Y-junction. Note also that, in practice, the height of the interaction arm is not uniform, and its actual maximum (which is reached at the arm center) equals the theoretical maximum only when the interaction arm is long enough, which happens when $k_3 - k_2$ is sufficiently small.

3.1.2. *Asymmetric 2-soliton interactions.* When $C = C_P$ in (11), it is $C_{1,4} = C_{2,3} = 0$ while all other minors are unity. The asymptotic solitons are [8, 19] and [17, 18], and the dominant phase combinations as $x \to -\infty$ and $x \to \infty$ are (3, 4) and (1, 2), respectively. Because the phase shift of the individual line solitons in asymmetric interactions has the opposite sign as that in ordinary interactions, however, in this case the interaction arm is the boundary between the two dominant regions in the limits $y \to \pm\infty$ with $x$ finite. The corresponding phase combinations are (1, 3) and (2, 4). Which one of these is dominant as $y \to \infty$ depends on the relative velocity of the two solitons, which is in general undetermined in asymmetric solutions. This, however, is irrelevant to our calculation. Thus, the amplitude of the interaction region is still given by $a_{13,24}$ as for ordinary solutions. What is different from before is the value of this amplitude relative to that of the individual solitons. Recall that, for asymmetric solutions, it is always $a_{2,3} < a_{1,4}$. It is trivial to see that $a_{13,24} = a_{1,4} - a_{2,3} < a_{1,4}$. Therefore, the amplitude of the interaction region in asymmetric solutions is always lower than that of the highest soliton. As to the other soliton, one can easily see that $a_{13,24} > a_{2,3}$ if and only if $a_{1,4} > 2a_{2,3}$.

3.1.3. *Resonant 2-soliton interactions.* For the coefficient matrix $C_T$ in (11) all minors are nonzero. The dominant phase combinations as $x \to -\infty$ and $x \to \infty$ are, respectively, (3, 4) and (1, 2), as with asymmetric solutions, but the asymptotic solitons here are [8, 18] and [17, 19]. Here the interaction is mediated by four interaction segments instead of just one, and the solution is nonstationary. (Its time evolution is shown in Figure 2.) Hence, the situation appears at first to be more complicated than in the other two cases. Nonetheless, the calculations are actually simpler, because all the intermediate arms are true line solitons of the KPII equation, and the resonance condition is satisfied at all vertices. Moreover, the interaction pattern obeys the reflection symmetry $(x, y, t) \to (-x, -y, -t)$. Indeed, it is trivial to see that, at all times, the tallest intermediate soliton is [8, 19], which is obviously taller than either of the asymptotic solitons. Note, however, that $a_{1,3} + a_{2,4} = a_{1,4} + a_{2,3} > a_{1,4}$. Thus the maximum interaction amplitude is always less than the sum of the amplitudes of the asymptotic solitons, unlike the case of ordinary interactions. In particular, in the case of equal-amplitude solitons, $a_{1,3} = a_{2,4} =: a$, we have $U_{\max} = \frac{1}{2}a_{1,4}^2 < 2a^2$. Thus the maximum height is less than four times that of the asymptotic solitons.

### 3.2. Inelastic 2-soliton interactions

Inelastic 2-soliton solutions fall into four categories [20], identified by the following coefficient matrices in RREF:

$$C_{\rm I} = \begin{pmatrix} 1 & 1 & 0 & -r \\ 0 & 0 & 1 & 1 \end{pmatrix}, \qquad C_{\rm II} = \begin{pmatrix} 1 & 0 & -r & -r \\ 0 & 1 & 1 & 1 \end{pmatrix},$$
$$C_{\rm III} = \begin{pmatrix} 1 & 0 & 0 & -r \\ 0 & 1 & 1 & 1 \end{pmatrix}, \qquad C_{\rm IV} = \begin{pmatrix} 1 & 0 & -r & -1 \\ 0 & 1 & 1 & 0 \end{pmatrix}, \tag{15}$$

with $r > 0$. We consider each of these in turn. Note that in all of these cases exactly one of the minors of $C$ is zero while all other minors are unity, which produces a tau function with five phase combinations. For simplicity in what follows we set $r = 1$.

3.2.1. *Type I*. In this case $C_{1,2} = 0$. The incoming solitons are [8, 17] and [17, 19], the outgoing solitons are [8, 18] and [18, 19]. The dominant phase combination as $x \to -\infty$ is (3, 4), while that as $x \to \infty$ is (1, 3). The interaction pattern is a combination of two Y-shape resonances, as shown in Figures 3 and 4. In particular, Figure 4 shows contour plots of the solution as well as the index pairs corresponding to each of the intermediate and

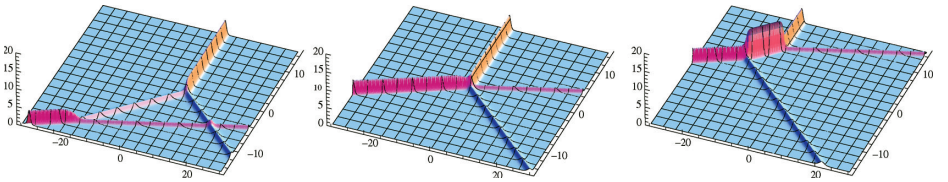

Figure 3. Time evolution of the inelastic 2-soliton solution obtained from the coefficient matrix $C_{\rm I}$ in (15) with $(k_1, \ldots, k_4) = (-2, 0, 2, 4)$. Left: $t = -2$; center: $t = 0$; right: $t = 2$.

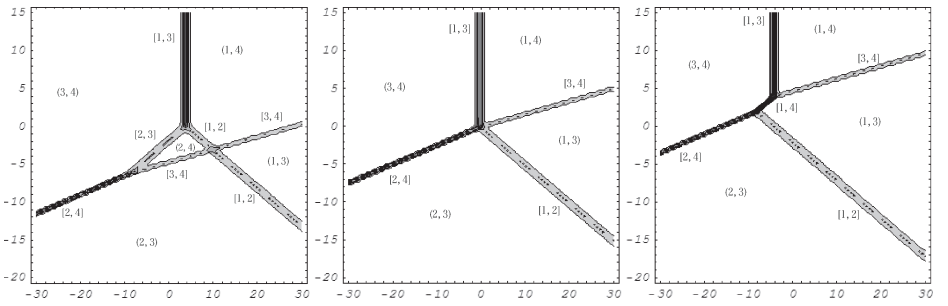


Figure 4. Contour plots of the inelastic 2-soliton solution shown in Figure 3. The dominant phase combinations $(m_1, m_2)$ and the index pairs $[i, j]$ that uniquely identify the line solitons are labeled. Left: $t = -1$; center: $t = 0$; right: $t = 1$.

asymptotic solitons. The interaction vertices, however, are not invariant: For $t < 0$ the three phases appearing at each interaction vertex are, respectively, (2, 3, 4) and (1, 2, 3), corresponding, respectively, to solitons [17, 18], [18, 19], [17, 19] and [8, 17], [17, 18], [8, 18]. But at $t = 0$ two resonant stems collide, and the arrangement of solitons changes thereafter, with the resonant vertices being characterized by the phases (1, 2, 4) and (1, 3, 4) for $t > 0$, corresponding, respectively, to solitons [8, 17], [8, 19], [17, 19] and [8, 18], [8, 19], [18, 19]. (An additional X-shape vertex is produced for $t < 0$ by the asymptotic solitons [8, 17] and [18, 19], which, as to be expected, interact nonresonantly.)

The rearrangement in the soliton configuration that happens at $t = 0$ corresponds to the generation of a large-amplitude wave for $t > 0$. The interaction arm is the intermediate soliton [17, 18] for $t < 0$ and [8, 19] for $t > 0$. The first of these is always shorter than the asymptotic solitons [8, 18] and [17, 19]. The second one, however, is taller than any of the others. Moreover, the height of the interaction arm [8, 19] is $U_{\max} = \frac{1}{2}a_{1,4}^2 = \frac{1}{2}(a_{1,j} + a_{j,4})^2 > \frac{1}{2}(a_{1,j}^2 + a_{j,4}^2)$, for $j = 2, 3$. Thus, the height of the soliton [8, 19] is always greater than the sum of the heights of the incoming and the outgoing solitons. As before, the maximum value of the interaction height relative to the height of the asymptotic solitons occurs in the case of equal amplitudes: when $a_{1,2} = a_{2,4} =: a$, it is $U_{\max} = 2a^2$, yielding a ratio of four to one.

3.2.2. *Type II*. In this case $C_{3,4} = 0$. The incoming solitons are [6, 17] and [17, 18], the outgoing solitons are [8, 19] and [17, 19]. The whole solution is a time reversal of the inelastic 2-soliton solution of type I: that is, $u_{\mathrm{II}}(x, y, t) = u_{\mathrm{I}}(-x, -y, -t)$. The dominant phase combination as $x \to -\infty$ and $x \to \infty$ are now, respectively, (2, 4) and (1, 2). The tall interaction arm is still the soliton [8, 19], but now it appears for all $t < 0$.

3.2.3. *Type III*. In this case $C_{2,3} = 0$. The incoming solitons are [8, 19] and [17, 18], the outgoing solitons are [8, 19] and [17, 19]. The dominant phase combination as $x \to -\infty$ is (3, 4), while that as $x \to \infty$ is (1, 2). The interaction dynamics is similar to that of solutions of type I, as shown in Figures 5 and 6.

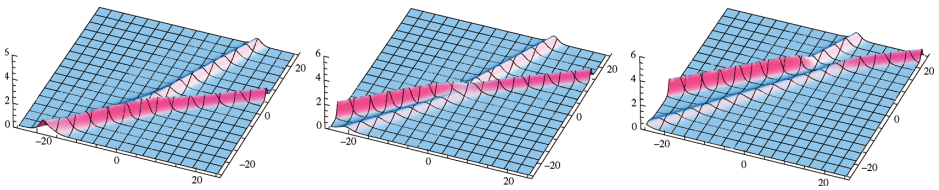

Figure 5. Time evolution of the inelastic 2-soliton solution obtained from $C_{\mathrm{III}}$ in (15) with $(k_1, \ldots, k_4) = (-0.5, -0.1, 1, 1.7)$. Left: $t = -5$; center: $t = 0$; right: $t = 5$.

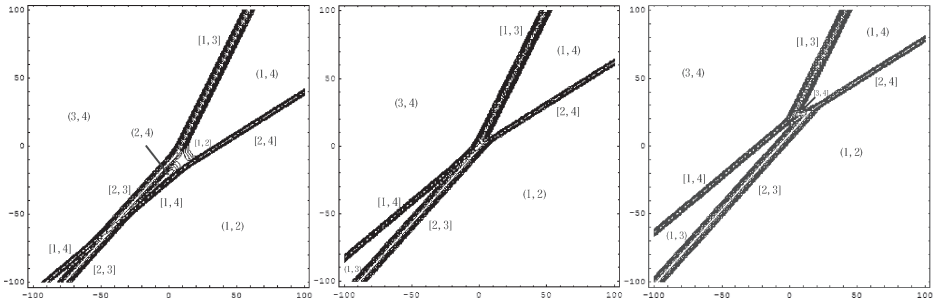


Figure 6. Contour plots of the time evolution of the inelastic 2-soliton solution shown in Figure 5. Left: $t = -13$; center: $t = 0$; right: $t = 10$.

In particular, the interaction arms for $t < 0$ and $t > 0$ are, Respectively, given by the double-phase transition $(1, 3) \leftrightarrow (2, 4)$ and by the single-phase transition $(1, 3) \leftrightarrow (1, 4)$. The first of these transitions produces the intermediate soliton [18, 19]; the second a double-soliton of the form (13). Note, however, that which one of these solitons arises at positive versus negative times is determined by the relative slope of the incoming solitons, which is determined by the specific values of the phase parameters $k_1, \ldots, k_4$ and is therefore undetermined in general, as in asymmetric 2-soliton solutions. The amplitude of the [18, 19] intermediate soliton is of course smaller than that of any asymptotic solitons. The amplitude of the double-soliton is $a_{13,24} = a_{1,2} + a_{3,4} = a_{1,4} - a_{2,3}$, and the corresponding height is $\frac{1}{2}a_{13,24}^2 = \frac{1}{2}(a_{1,4} - a_{2,3})^2 < \frac{1}{2}a_{1,4}^2$. This height, however, is smaller than that of the incoming asymptotic solitons.

3.2.4. *Type IV*. In this case $C_{1,4} = 0$. The incoming solitons are [8, 18] and [17, 19], the outgoing solitons are [8, 19] and [17, 18]. Such a solution and is a time-reversal version of the inelastic solution of type III: that is, $u_{\mathrm{IV}}(x, y, t) = u_{\mathrm{III}}(-x, -y, -t)$.

### *3.3. Generation of large-amplitude waves*

None of the three types of elastic 2-soliton solutions describes the generation of large-amplitude waves from the interaction of lower-amplitude ones, because the interaction pattern of ordinary and asymmetric solutions is stationary, and the intermediate soliton [8, 19] in resonant solutions is present at all times. On the other hand, inelastic solutions of type I do have the effect of an amplification of the maximum wave height. Moreover, when this kind of solution is embedded in a larger soliton complex, further increases of the wave height may result from the interaction of the interaction arm with the other solitons in the complex. As an example, Figure 7 shows the large-amplitude

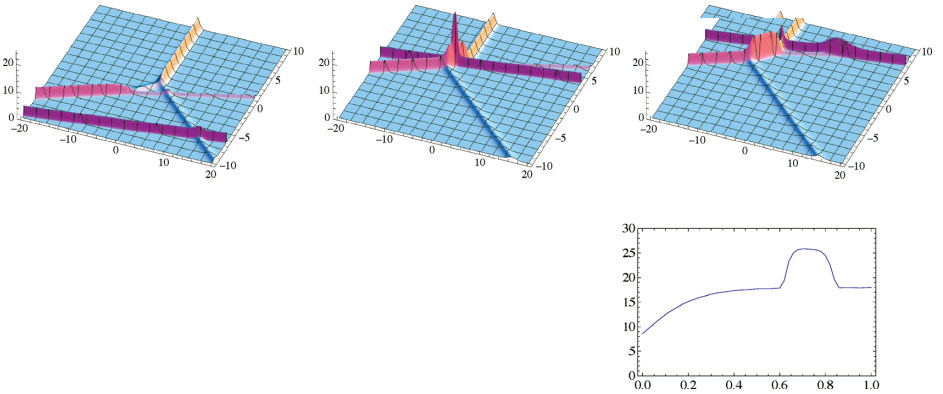

Figure 7. A solution of KP generating an extreme wave, as produced by the coefficient matrix in (16) with $(k_1, \ldots, k_6) = (-2,\ 0,\ 2,\ 4,\ 4.1,\ 8), \theta_{1;0} = \ldots \theta_{5;0} = 0$ and $\theta_{6;0} = 200$. Above, left: $t = -0.4$; above, center: $t = 0.7$; above, right: $t = 1$. Bottom right: the maximum wave height as a function of time.

wave produced by the interaction generated by the $3 \times 6$ coefficient matrix

$$C = \begin{pmatrix} 1 & 1 & 1 & 0 & 0 & 0 \\ 0 & 0 & 1 & 1 & 0 & 0 \\ 0 & 0 & 0 & 0 & 1 & 1 \end{pmatrix}. \tag{16}$$

As evident from Figure 7, the interaction among the solitons results in the temporary generation of an extreme wave whose height is several times larger than the sum of the heights of the interacting waves.

This discussion suggests the following physical mechanism of generation of extreme waves: (i) several solitons are generated by external sources; (ii) two of those solitons generate a large-height interaction arm, as in the case of ordinary 2-soliton solution solutions, or that of inelastic solutions of type I; (iii) this interaction arm interacts with one of the other solitons or interaction arms, in which case the wave height can be many times higher that of each asymptotic soliton; (iv) after the interaction, the wave amplitude decreases.

### *3.4. A method to predict maximum interaction amplitudes*

The above results yield a method to predict the possible maximum amplitude of a soliton interaction based only on information about the asymptotic line solitons. Consider first the case in which there are two line solitons as $y \to \pm\infty$. Let $(a_1^-,\ d_1^-)$ and $(a_2^-,\ d_2^-)$ be the amplitudes and directions of the incoming line solitons, and $(a_1^+,\ d_1^+)$ and $(a_2^+,\ d_2^+)$ be those of the outgoing line solitons, both sorted in order of increasing values of $d$. If $d_1^- = d_1^+$ or $d_2^- = d_2^+$, the incoming and outgoing line solitons coincide, implying that one has an elastic soliton interaction. Otherwise one has an inelastic soliton

interaction. For an elastic soliton interaction, the interaction amplitude is computed as follows. Let $\kappa_{n,\pm} = (d_n \pm a_n)/2$ for $n = 1, 2$. [The superscript $\pm$ in the soliton parameters $a_n$ and $d_n$ can of course be dropped for elastic solutions.] Then define the phase parameters $k_1, \ldots, k_4$ to be the values $\kappa_{1,\pm}$, $\kappa_{2,\pm}$ rearranged in order of increasing size, such that $k_1 < k_2 < k_3 < k_4$. In this way each soliton is uniquely identified by the index pair $[i_n, j_n]$ that labels the position of $\kappa_{n,-}$ and $\kappa_{n,+}$ (respectively) in the list $k_1, \ldots, k_4$. The type of index overlap determines the type of soliton interaction [17, 20, 21], and the interaction amplitude is then obtained from the calculations described earlier. A similar method applies in the case of an inelastic interaction. In this case, however, one needs the asymptotic data both as $y \to -\infty$ and as $y \to \infty$ to uniquely identify the type of interaction.

If the number of solitons is greater than two, one selects any two neighboring solitons and perform the above procedure to compute the possible maximum amplitude. One then repeats these steps for all possible pairwise combinations of solitons. Note, however, that, unlike the case of two solitons, this procedure does not yield a precise estimate, for two reasons: (i) whether or not the theoretical maximum amplitude in each pairwise interaction is realized depends on the details of the soliton configuration; (ii) these high-amplitude intermediate solitons resulting from pairwise interactions can in some cases interact among themselves producing solitons of even higher amplitude. Again, whether or not this happens depends on the details of the soliton configuration. A true upper bound can be obtained: $U_{\max} = \frac{1}{2}(k_{\max} - k_{\min})^2$. This theoretical maximum, however, is realized only in a small number of soliton interactions, as should already be evident from the case of 2-soliton solutions.

## 4. Numerical simulations

We now describe numerical simulations of multi-soliton interactions of the KPII equation. The numerical simulation of multi-soliton solutions is particularly important, because at present no analytical methods exist to investigate the stability of such solutions using either the inverse scattering transform or other techniques.

### *4.1. A computational method for line-soliton solutions*

The numerical integration of the KP equation poses a number of challenges (e.g., see [29] and references therein). In particular, when simulating soliton solutions one must take into account that line solitons are not localized objects, but they extend through the boundaries of any finite computational window. The approach we used here is based on the one in [30–34], but with different boundary conditions. For the $x$-direction, we set our computational

window to be wide enough that any initial solitary waves are far away from boundary. This allows us to use periodic boundary conditions and to compute $x$-derivatives with spectral methods. For the $y$-direction we employ the windowing method [35], which has its roots in signal processing, and where the windowing operation allows the spectral analysis of nonperiodic signals. We use the following window function: $W(y) = 10^{-a^n|2y/L-1|^n}$, where $L$ is the length of the computational window in the $y$-direction, and $a$ and $n$ are parameters. Here we set $a = 1.111$ and $n = 27$. We then transform the solution as follows:

$$q(x, y, t) = W(y)\, u(x, y, t)\,, \qquad Q(x, y, t) = W(y)\, u^2(x, y, t)\,. \tag{17}$$

Substituting this into the KPII equation, we obtain

$$\left(-4q_t + 3Q_x + q_{xxx}\right)_x + 3q_{yy} - 6W_y u_y + 3W_{yy} u = 0\,. \tag{18}$$

All terms in this equation vanish at the boundaries in the $y$-direction. This makes it possible to apply pseudospectral methods to compute $y$-derivatives. We then integrate (18) in time in the Fourier domain using Crank–Nicholson differencing and an iterative method. Once $q(x, y, t)$ is obtained, $u(x, y, t)$ is recovered from (17). But note that the formula for $u(x, y, t)$ becomes ill-conditioned near the boundaries in the $y$-direction, where $W(y)$ tends to zero. Near these boundaries, we thus correct the solution using information about the soliton behavior. All the simulations were performed on a grid with $8192 \times 1024$ points, $\Delta x = \Delta y = 0.1$ and $\Delta t = 0.005$. Figures 8–11 later show the resulting field $q(x, y, t)$. Note that, to make the interactions more evident, only a small portion of the computational domain is often shown.

### *4.2. Numerical simulations of line-soliton interactions*

Figure 8 shows the field $q(x, y, t)$ corresponding to the numerical time evolution of an initial condition (IC) consisting of an exact fully resonant

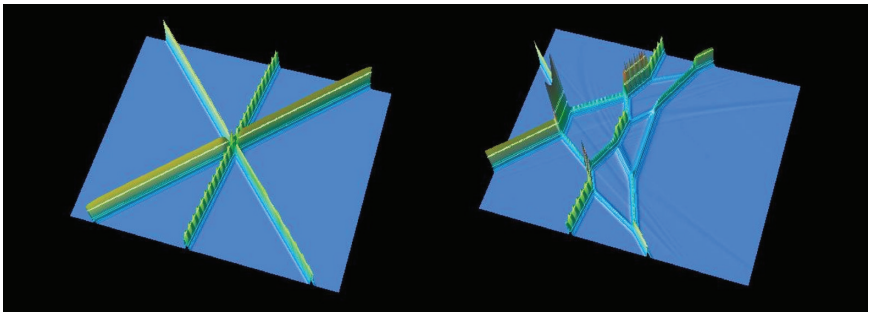

Figure 8. Numerical time evolution of the fully resonant 3-soliton interaction; $(k_1, \ldots, k_6) = (-2.5, -1.5, -0.5, 0.5, 1.5, 2.5)$. Left: $t = 0$; right: $t = 10$.

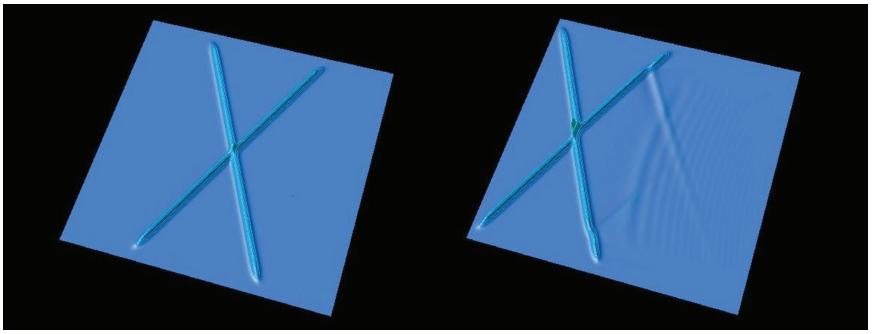

Figure 9. Numerical time evolution of a linear superposition of line solitons generating an ordinary 2-soliton interaction; $(k_1, \ldots, k_4) = (-1, -0.001, 0, 1)$. Left: $t = 0$; right: $t = 50$. The IC is not an exact 2-soliton solution, and some dispersive waves are generated, but the results suggest the stability of the soliton interactions.

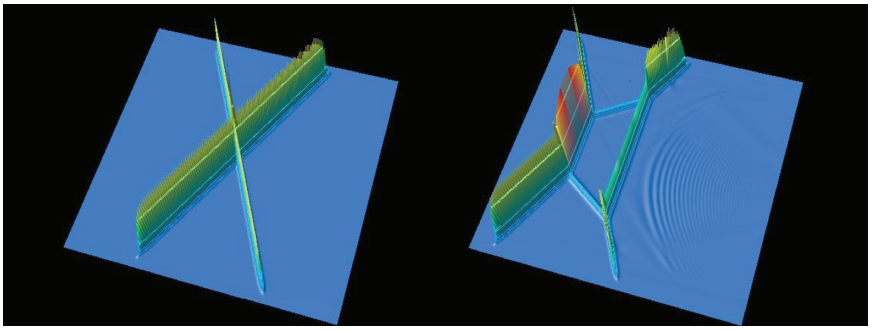

Figure 10. Numerical time evolution of a linear superposition of line solitons generating a resonant 2-soliton interaction; $(k_1, \ldots, k_4) = (-2, -1, 1, 2)$. Left: $t = 0$; right: $t = 12.5$. Again, dispersive waves are generated, but the interaction appears to be stable.

3-soliton solution. As evident from the figure, the numerical solution accurately reproduces the web structure observed in the exact solution. This result confirms that the numerical method described above can indeed effectively simulate multi-soliton interactions, and at the same time provides a first indication that such solutions are stable.

Next we describe the time evolution of ICs consisting of a linear superposition of two line solitons. Figures 9 and 10 show the cases where the amplitudes and directions were chosen so as to correspond, respectively, to an ordinary and resonant interaction. We emphasize that, in both cases, the initial state is not an exact two-soliton solution. Indeed, in both cases the numerical solution shows the presence of radiative component of small amplitude. Nonetheless, the results do provide a further check of the stability of 2-soliton interactions. Note in particular that the characteristic "box" of the resonant solution is generated numerically. Similar results were obtained by numerically computing

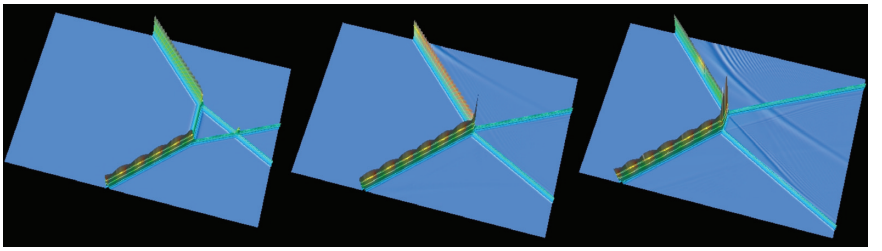

Figure 11. Numerical time evolution of an inelastic 2-soliton interaction. Left: $t = 0$; center: $t = 2.5$; right: $t = 5$.

the time evolution of an IC consisting of a linear superposition of two line solitons corresponding to an asymmetric interaction and of three line solitons corresponding to a fully resonant solution. Finally, Figure 11 shows the time evolution of an IC corresponding to an inelastic interaction.

Importantly, when the IC is not an exact 2-soliton solution, the numerical solutions show that the height of the interaction arm tends monotonically in time to the value for the corresponding exact soliton as obtained in Section 3, for example, in Figure 9 the height of interaction arm increases monotonically in time from its initial value of 2 [owing to an IC that is just a linear superposition of two line solitons], approaching asymptotically the value corresponding to ordinary 2-soliton interactions. Conversely, for an asymmetric solution the height of the interaction arm decreases in time, again approaching asymptotically the value for asymmetric 2-soliton interactions. These results extend the validity and usefulness of the analysis in Section 3.

The above results suggest that multi-soliton solutions of KPII are robust and stable, and moreover, that even when the solution contains nonsolitonic components, only the information about the asymptotics line solitons contributes to determine the intermediate interactions of the line solitons. We also suspect that, as the radiative components disperse, asymptotically in time the solution will be closely approximated by an exact soliton solution, similarly to the case of $(1 + 1)$-dimensional soliton equations. Of course all of these conjectures must be carefully tested and validated with extensive numerical simulations, which are beyond the scope of this work.

## 5. Conclusions

We have studied the amplitude of soliton interactions of the KPII equation, and we have discussed a possible mechanism for the generation of large-amplitude waves. Ordinary $N$-soliton interactions with $N \geq 3$ can also briefly produce large amplitude waves if all the solitons intersect simultaneously at the same point in the $xy$-plane. Note however that the event of all solitons intersecting

simultaneously at a single point can be considered to be statistically speaking unlikely in a multi-soliton complex, with a likelihood decreasing as the number of solitons increases. In this sense, therefore, the mechanism described in this paper, involving inelastic 2-soliton solutions (possibly embedded in a larger soliton complex, as in Figure 7) represents the most likely way to generate large-amplitude waves.

We also proposed a method to determine the maximum amplitude resulting from the interaction of two line solitons. The calculation of the maximum amplitude is based on the framework of exact line-soliton solutions, but it may also be useful for solutions where a nonsolitonic component is present, if line-soliton solutions of KPII are indeed proven to be stable, since then, even if one starts from an initial state that is not an exact soliton solution, the radiative portions of the solutions will disperse away, and asymptotically in time one will approach a state consisting of an exact soliton solution. An interesting open problem will be to develop an algorithm to compute the actual maximum amplitude generated by any multi-soliton configuration.

Finally, we implemented an algorithm to numerically integrate solutions of the KPII equation containing multi-soliton complexes, and we discussed the results of numerical simulations. These results show the robustness of all types of line-soliton solutions of KPII, including those exhibiting web-like structure. We also confirmed numerically that multi-soliton interactions can generate large amplitude waves, and that an initial state that is not an exact solution eventually converges to an exact multi-soliton solution. We note that resonant 2-soliton solutions with a hole have also been found in other discrete and continuous $(2 + 1)$-dimensional soliton equations [27, 30, 36–38], both in exact solutions and in numerical simulations, indicating that they are a fundamental and robust structure of $(2 + 1)$-dimensional soliton equations.

## Acknowledgments

We thank H. Segur for many interesting discussions. KM also acknowledges partial support from the twenty-first century COE program "Development of Dynamic Mathematics with High Functionality" at the Faculty of Mathematics, Kyushu University and Grant-in-Aid for Scientific Research from the Japan Society for the Promotion of Science.

## References

1. M. Hamer, Freak waves threaten Europe's coastline, *New Scientist 2201* 163:18 (1999).
2. C. Kharif and E. Pelinovsky, Physical mechanisms of the rogue wave phenomenon, *Euro. J. Mech. B* 22:603–634 (2003).
3. Y. Li and P. D. Sclavounos, Three-dimensional nonlinear solitary waves in shallow water generated by an advancing disturbance, *J. Fluid Mech.* 470:383–410 (2002).

4. E. Pelinovsky, T. Talipova, and C. Kharif, Nonlinear-dispersive mechanism of the freak wave formation in shallow water, *Physica D* 147:83–94 (2000).
5. A. V. Porubov, H. Tsuji, I. V. Lavrenov, and M. Oikawa, Formation of the rogue wave due to non-linear two-dimensional waves interaction, *Wave Motion* 42:202–210 (2005).
6. T. Soomere, Fast ferry traffic as a qualitatively new forcing factor of environmental processes in non-tidal sea areas: A case study in Tallinn Bay, Baltic Sea, *Env. Fluid Mech.* 5:293–323 (2005).
7. B. B. Kadomtsev and V. I. Petviashvili, On the stability of solitary waves in weakly dispersing media, *Sov. Phys. Dokl.* 15:539–541 (1970).
8. M. J. Ablowitz and H. Segur, *Solitons and the Inverse Scattering Transform*, SIAM, Philadelphia, PA, 1981.
9. H. Segur and A. Finkel, An analytical model of periodic waves in shallow water, *Stud. Appl. Math.* 73:183–220 (1985).
10. P. Peterson, T. Soomere, J. Engelbrecht, and E. van Groesen, Soliton interaction as a possible model for extreme waves in shallow water, *Nonlin. Proc. Geophys.* 10:503–510 (2003).
11. T. Soomere, Interaction of Kadomtsev-Petviashvili solitons with unequal amplitudes, *Phys. Lett. A* 332:74–81 (2004).
12. T. Soomere and J. Engelbrecht, Extreme elevations and slopes of interacting solitons in shallow water, *Wave Motion* 41:179–192 (2005).
13. J. W. Miles, Obliquely interacting solitary waves, *J. Fluid Mech.* 79:157–169 (1977).
14. J. W. Miles, Resonantly interacting solitary waves, *J. Fluid Mech.* 79:171–179 (1977).
15. M. Oikawa and H. Tsuji, Oblique interactions of weakly nonlinear long waves in dispersive systems, *Fluid Dyn. Res.* 38:868–898 (2006).
16. G. Biondini and Y. Kodama, On a family of solutions of the Kadomtsev Petviashvili equation which also satisfy the Toda lattice hierarchy, *J. Phys. A* 36:10519–10536 (2003).
17. G. Biondini, Line soliton interactions of the Kadomtsev-Petviashvili equation, *Phys. Rev. Lett.* 99:064103-1–064103-4 (2007).
18. G. Biondini and S. Chakravarty, Soliton solutions of the Kadomtsev-Petviashvili II equation, *J. Math. Phys.* 47:033514-1–033514-26 (2006).
19. G. Biondini and S. Chakravarty, Elastic and inelastic line-soliton solutions of the Kadomtsev-Petviashvili II equation, *Math. Comp. Sim.* 74:237–250 (2007).
20. S. Chakravarty and Y. Kodama, Classification of the line-soliton solutions of KPII, *J. Phys. A* 41:275209–275241 (2008).
21. Y. Kodama, Young diagrams and N-soliton solutions of the KP equation, *J. Phys. A* 37:11169–11190 (2004).
22. R. Hirota, *The Direct Method in Soliton Theory*, Cambridge University Press, Cambridge, U.K., 2004.
23. J. Satsuma, N-solution of the two-dimensional Korteweg-deVries equation, *J. Phys. Soc. Jpn.* 40:286–290 (1976).
24. N. C. Freeman, Soliton interactions in two dimensions, *Adv. Appl. Mech.* 20:1–37 (1980).
25. N. C. Freeman and J. J. C. Nimmo, Soliton solutions of the Korteweg-deVries and the Kadomtsev-Petviashvili equations—The wronskian technique, *Phys. Lett. A* 95:1–3 (1983).
26. E. Medina, An N soliton resonance solution for the KP equation: Interaction with change of form and velocity, *Lett. Math. Phys.* 62:91–99 (2002).

27. E. Infeld and G. Rowlands, *Nonlinear Waves, Solitons and Chaos*, Cambridge University Press, Cambridge, 2000.
28. M. Boiti, F. Pempinelli, A. K. Pogrebkov, and B. Prinari, Towards an inverse scattering theory for non-decaying potentials of the heat equation, *Inv. Probl.* 17:937–957 (2001).
29. C. Klein, C. Sparber, and P. Markowich, Numerical study of oscillatory regimes in the Kadomtsev-Petviashvili equation, *J. Nonlin. Sci.* 17:429–470 (2007).
30. H. Tsuji and M. Oikawa, Two-dimensional interaction of internal solitary waves in a two-layer fluid, *J. Phys. Soc. Jpn.* 62:3881–3892 (1993).
31. H. Tsuji and M. Oikawa, Oblique interaction of internal solitary waves in a two-layer fluid of infinite depth, *Fluid Dyn. Res.* 29:251–267 (2001).
32. H. Tsuji and M. Oikawa, Two-dimensional interaction of solitary waves in a modified Kadomtsev-Petviashvili equation, *J. Phys. Soc. Jpn.* 73:3034–3043 (2004).
33. H. Tsuji and M. Oikawa, Oblique interaction of solitons in an extended Kadomtsev-Petviashvili equation, *J. Phys. Soc. Jpn.* 76:084401-1–084401-8 (2007).
34. S. B. Wineberg, J. F. McGrath, E. F. Gabl, L. R. Scott, and C. E. Southwell, Implicit spectral methods for wave propagation problems, *J. Comp. Phys.* 97:311–336 (1991).
35. P. Schlatter, N. A. Adams, and L. Kleiser, A windowing method for periodic inflow/outflow boundary treatment of non-periodic flows, *J. Comp. Phys.* 206:505–535 (2005).
36. F. Kako and N. Yajima, Interaction of ion-acoustic solitons in two-dimensional space, *J. Phys. Soc. Jpn.* 49:2063–2071 (1980).
37. Y. Kodama and K.-I. Maruno, N-soliton solutions to the DKP equation and Weyl group actions, *J. Phys. A* 39:4063–4086 (2006).
38. K.-I. Maruno and G. Biondini, Resonance and web structure in discrete soliton systems: The two-dimensional Toda lattice and its fully discrete and ultra-discrete analogues, *J. Phys. A* 37:11819–11839 (2004).

State University of New York, Buffalo
University of Texas-Pan American
Kyushu University
Kyushu University

(Received December 5, 2008)